N O T E

The Maxwell Wheel Investigated with MBL

Barbara Pecori, Physics Department, Bologna University, Bologna, Italy; Pecori@gpxbof.df.unibo.it, *and*
Giacomo Torzo, Physics Department, Padova University, Padova, Italy; Torzo@padova.infm.it

The Maxwell wheel is a device traditionally used in the introductory physics lab to investigate the moment of inertia of a disc. The apparatus consists of a disc of radius R having an axis of radius r (with r << R) suspended from a fixed frame by two strings of equal length, which are wound around the axis (see Fig. 1).[1] There are several obvious features of the motion of the Maxwell wheel. First we see that the velocity and therefore the acceleration of the "fall" are smaller than those of a free falling body. Second, we see that the disc rotates. More precisely, to fall it must rotate, and when it reaches the end of the string, it must climb up in order to maintain its angular momentum. Finally, we notice that in its lowest position the disc stretches the strings.

This paper illustrates the didactic advantages of a *kinematic* and *dynamic* study of the Maxwell wheel motion with modern sensors in a microcomputer-based lab.

Experimental Setup

By interfacing a Maxwell wheel to a Personal Computer (PC) through a position sensor (sonar) and a force sensor (Fig. 2), the system evolution in time may be observed and recorded both *kinematically* (from *position* measurements *velocity* and *acceleration* are calculated) and *dynamically* (the force transducer measures the wire *tension*).

We use two types of low-cost interfaces specially suitable for didactic applications (ULI II[2] and PASCO[3] 500), both bundled with software designed for easy data acquisition and handling. The interface communicates with the PC through the slow RS232 serial port (COM in Windows and AppleTalk in Macintosh), but an internal buffer memory allows the collection of data at a high rate.

Our Maxwell wheel (shown in Fig. 3) is made from a thin metal disc of radius R with a central hole hosting an axis that has three sections with different diameters (4.0, 6.3, and 8.0 mm) to give three values for the ratio R/r. At both ends of each section thin transverse holes (1 mm) are drilled for attaching the strings.

Example of Motion Acquisition

Using a brass wheel of radius R = 47.5 mm, thickness 3 mm, and mass m = 227 g, with axis radius r = 2 mm, we obtained the plots shown[4] in Fig. 4. Note how the position-versus-time plot (A) resembles that of a bouncing ball. The velocity plot (B) shows discontinuities corresponding to the "bounces," where the velocity suddenly changes sign. Plot (C) shows that the acceleration is negative and small during climb and fall, with positive peaks at the bottom positions. The force plot (D) shows that the string tension has corresponding peaks.

Physical Descriptions

The simplest model is based on energy considerations. If we let the

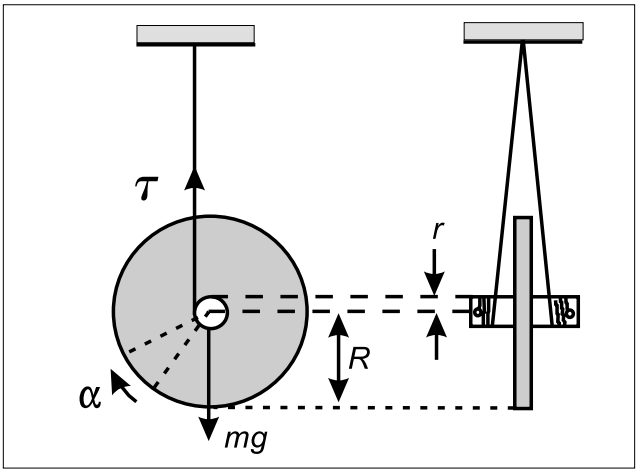

Fig. 1.

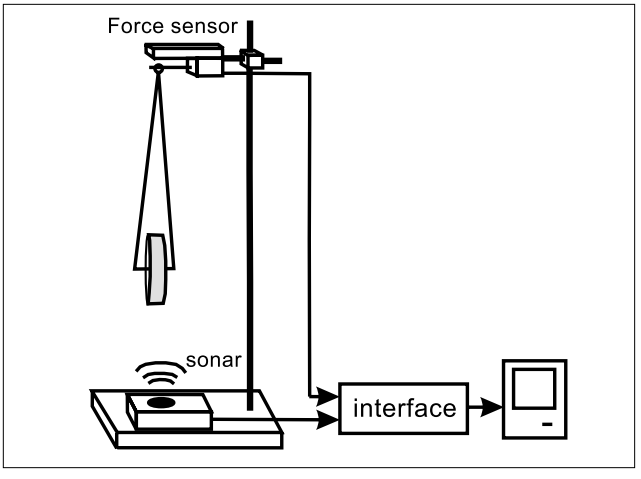

Fig. 2.

wheel fall from a height h, and the potential energy $U(x)$ is referred to the equilibrium position ($U = 0$ at $x = 0$), the system total energy E at the start ($x = h$, $v = 0$) is $E = mgh$. During the fall the *potential* energy transforms into *translational kinetic* energy $E_t = \frac{1}{2}mv^2$ and *rotational kinetic* energy $E_r = \frac{1}{2}I\omega^2$. Assuming negligible dissipation, we may write therefore: $E = U(x) + E_t(x) + E_r(x)$, or $mgh = mgx + \frac{1}{2}mv^2 + \frac{1}{2}I\omega^2$, where m is the Maxwell wheel mass, I the moment of inertia, and ω the angular velocity. This energy balance explains why the linear acceleration is less than g. To experimentally test the model, we should write the acceleration as a function of directly measurable quantities. To do this we exploit the fact that the translational and rotational motions are not independent.

Using an upward vertical axis with the origin in the equilibrium position, the rotation angle $\alpha(t)$ is related to the displacement $x(t)$ by: $x(t) = r\,\alpha(t)$ (where r is the axis radius), while the angular velocity is related to the linear velocity by:

$$v(t) = r\omega(t) \qquad (1)$$

We may therefore write all the quantities as functions of *position* x and of *velocity* v so that the energy balance becomes:

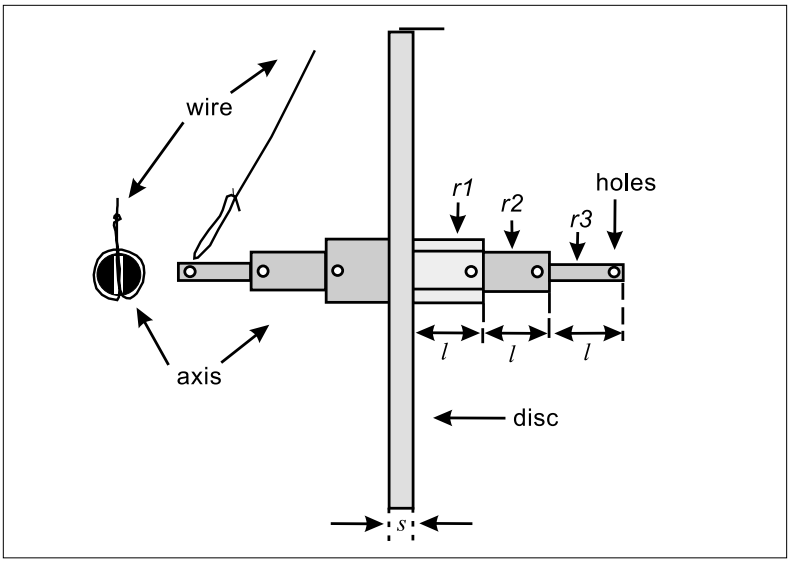

Fig. 3.

$$mg(h - x) = \tfrac{1}{2}mv^2 + \tfrac{1}{2}I\omega^2 = \frac{1}{2}m\left(1 + \frac{I}{mr^2}\right)v^2 = \frac{1}{2}(mk)v^2$$

showing that the system behaves like a point with inertial mass $mk = m(1 + I/mr^2)$. Solving with respect to the velocity, we get a relation similar to that for the velocity of a free body falling from height h:

$$v(x) = \sqrt{\frac{2g(h-x)}{1 + I/(mr^2)}} = \sqrt{2\frac{g}{k}(h-x)}$$

$$= \sqrt{2a(h-x)}$$

showing that the acceleration of the center of mass is[5]

$$a = g/k = g/(1 + I/mr^2) \qquad (2)$$

For $r << R$, the moment of inertia, I, of the wheel is a good approximation to that of the disc ($I \approx mR^2/2$), and therefore the predicted acceleration is

$$a \approx g/\left(1+R^2/2r^2\right) \approx g\left(2r^2/R^2\right) \qquad (3)$$

Checking Predictions

The moment of inertia of a homogeneous cylinder of density ρ, radius R, and length s is $I = \pi R^4 s\rho/2$. For our Maxwell wheel, made of four cylinders, we get:

$$I = (\pi\rho/2)[R^4 s + (r_1^4 + r_2^4 + r_3^4)2\ell]$$

$$= (\pi\rho R^4 s/2)\left[1 + \left\{\frac{r_1^4 + r_2^4 + r_3^4}{R^4}\,\frac{2\ell}{s}\right\}\right]$$

With $R = 47.5$ mm, $s = 3.0$ mm, $r_1 = 4.0$ mm, $r_2 = 3.2$ mm, $r_3 = 2.0$ mm, and $l = 20$ mm, the term within curl brackets is negligible (1.9×10^{-3}), and we may therefore approximate I with the moment of inertia of the disc only: $I \approx mR^2/2$, letting $k \approx (R/r)^2/2$.

With the values chosen in the setup of Fig. 4, the predicted values were $k \approx 283$ and $a = 0.035$ m/s^2. The experimental value $a = 0.044$ m/s^2,

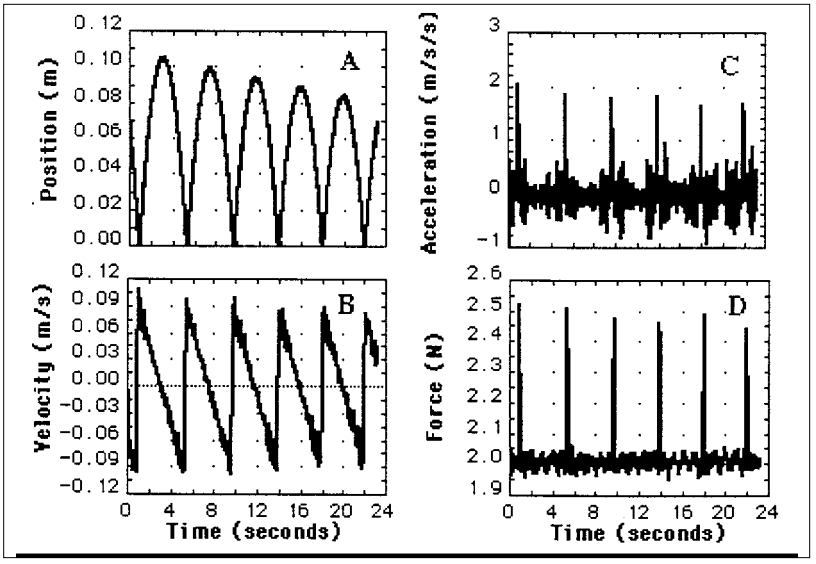

Fig. 4.

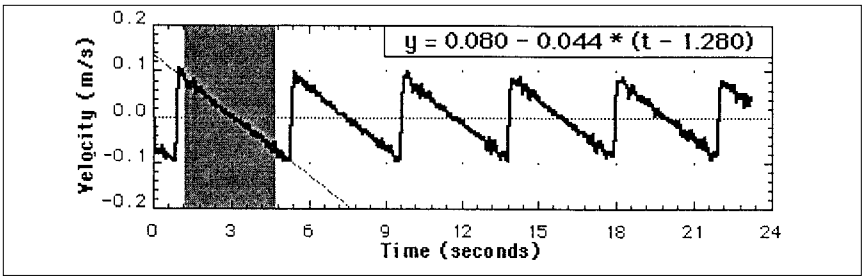

Fig. 5.

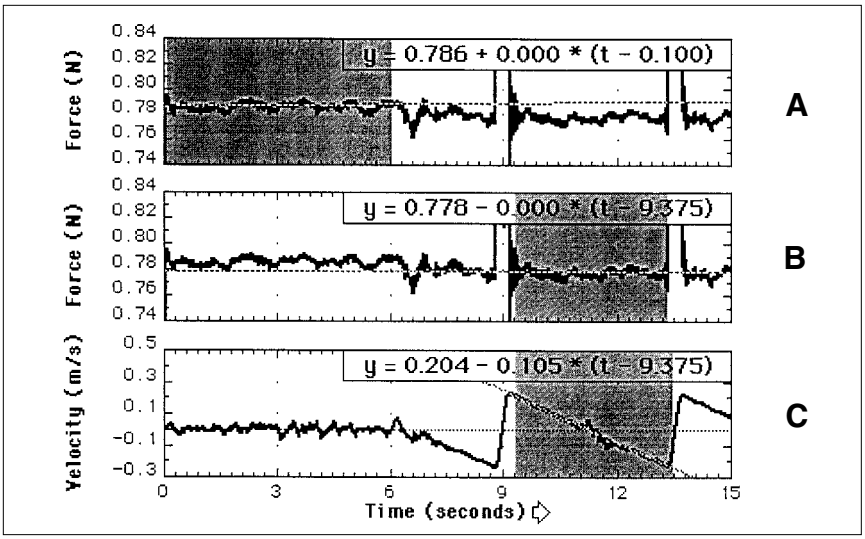

Fig. 6.

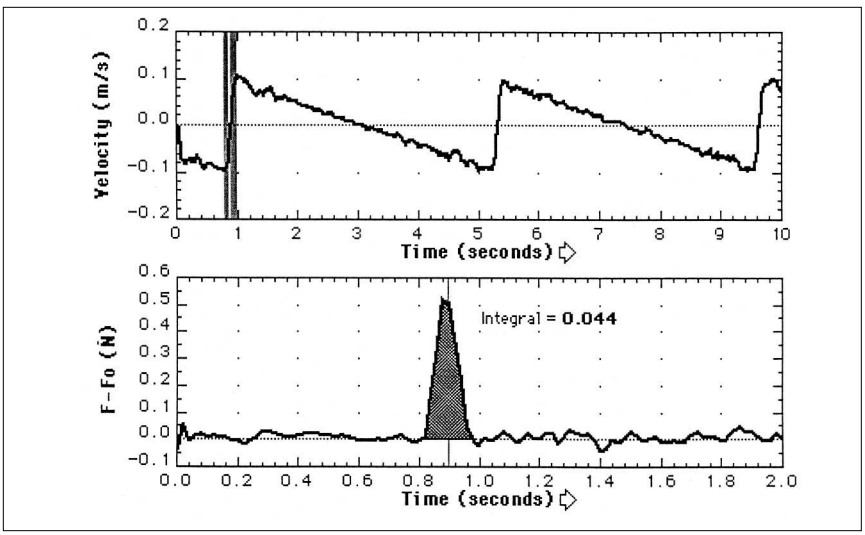

Fig. 7.

obtained by fitting linearly the velocity data (see Fig. 5), has the predicted order of magnitude, but is in excess by more than 20%. Therefore we must conclude that in our model we neglected some important feature of the studied phenomenon. Observe that we assumed a zero thickness of the string, which in our case is (0.40 ± 0.05) mm. The effective value of the axis radius must be increased by about half of the string thickness (0.2 mm). This lowers the k value to 232 ± 10, and the predicted value of the acceleration becomes a = 0.042 ± 0.002 ms^2, agreeing very well with the experimental result.

The finite string thickness introduces a correction of 18% (much greater than that due to the moment of inertia of the wheel axis ≈ 0.2%). This tells us that details that at first sight seem negligible may turn out to be quite important.

"Static" and "Dynamic" Disc Weight

The force sensor records the sum of the vertical components of the wire tensions, revealing, for example, a change when, having immobilized the disc with an extra string, we cut it and let the wheel fall. In our model the tension measured with the steady disc must equal the weight $\tau_o = mg$, and with the falling disc it must be $\tau_1 = mg - ma$. With an aluminum disc of 80 g, the static tension is τ_o = 0.786 N and the predicted difference is $\Delta\tau = \tau_o - \tau_1 = ma$ = (0.08 kg) x (0.1 ms^{-2}) ≈ 0.008 N, the value for a being obtained from the experimental data (see Fig. 6C). Here we recommend the use of a larger axis radius (r = 3.2 mm) to make the acceleration larger in order to make the variation detectable.

Recording the force before and after cutting the string,[6] we get tension values τ_o = 0.786 N and τ_1 = 0.778 N (see Fig. 6B) whose difference is consistent with the expected value.

"Collision" at the End of the String

When the Maxwell wheel reaches the end of the string, it has a momentum mv directed *downward*. This downward motion is stopped and reversed by the *string stretching*, which mimics a *collision* against an "invisible wall." The collision at the end of the string takes place within a short time (Δt ≈ 0.16 s). During this time the translational kinetic energy is first converted into elastic energy, stored within the stretched string (and the strained force sensor), and then given back again as translational kinetic energy now associated with an *upward* motion.

Newton's second law relates the momentum change to the impulsive

force $f_i(t)$: in differential form $f_i = ma = m(dv/dt)$, in integral form $m\Delta v = \int f_i(t)dt$. The impulsive force here is the change $\tau - \tau_o$ of the string's tension, measured by the force sensor.

Figure 7 shows, on an expanded timescale, the same data as in Fig. 5 in order to compare the momentum change, $\Delta(mv)$, with the integral of the pulse, $f_i dt$. The integral, computed by the dedicated software as the area under the curve $\tau(x) - \tau_o$, gives the value 0.044 Ns, very close to the value of the product $m(v_2 - v_1)$ = (0.227 kg) x (0.2 m/s^2) = 0.045 Ns.

Energy vs Time

The total energy of the wheel during the upward and downward motion may be calculated from the measured values of position x and velocity v of the center of mass:

$$E(x,v) = mgx + \frac{1}{2}mv^2 + \frac{1}{2}I\omega^2$$
$$= mgx + \frac{1}{2}m\left(1 + \frac{I}{mr^2}\right)v^2$$
$$= mg(x + v^2/2a) \qquad (4)$$

where we use relation (2) to express I/mr^2 in terms of g and a (calculated from experimental data as in Fig. 8A). The calculated values of the total energy, plotted versus time in Fig. 8B, show that the sum of the potential and kinetic energy during each cycle of the downward and upward motion is almost constant, as expected. In this plot energy seems to disappear during the collisions. This is due to two different limitations in the way total energy has been computed. The first is that relation (4) is based on relation (1), which is not valid when x reaches values close to zero; i.e., during the collision at the string's end. In fact, during the string's stretching the linear velocity changes sign (passing through zero) while the angular velocity remains approximately constant. The second limitation is that relation (4) does not take into account the elastic energy of the stretched string.

Keeping the two limitations in mind, we find (Fig. 8B) that during upward and downward motion the total energy decrease can be fitted exponentially (with a time constant of about 55 s). Since the decrease appears to occur uniformly during the whole motion it seems mainly due to viscous friction.

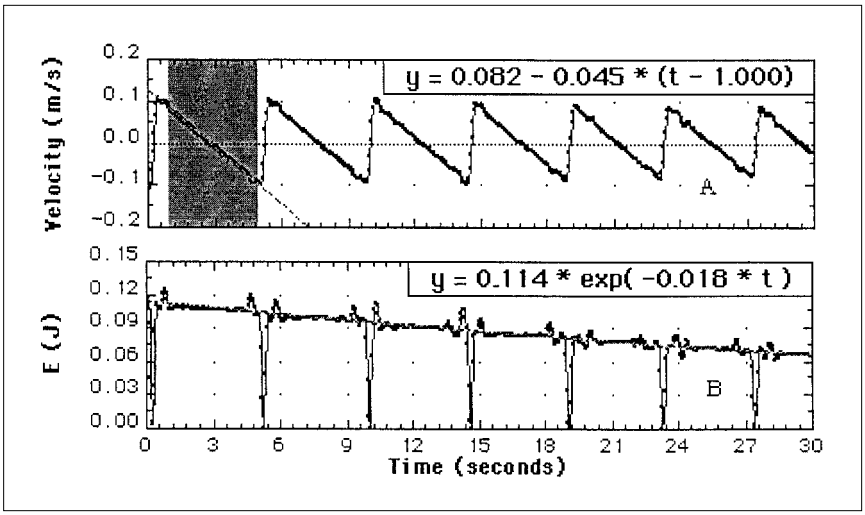

Fig. 8.

Suggestions for Teaching

A more familiar version of the Maxwell wheel is the traditional toy yo-yo. The experimental setup already described can be used for the experimental investigation of the behavior of a yo-yo, which may prove a good start for the study of translational and rotational motions. A record of the experimental data we obtained with a commercial yo-yo (a plastic toy with mass m = 18 g and axis radius r = 3.5 mm) is shown in Fig. 9.

To compare the model predictions with the experimental results, we should know r, m, and I. But for a yo-yo it is difficult to evaluate the moment of inertia, since its shape is not a geometrically simple one. However, it may be fruitful to use the plots in order to try a qualitative check of our model. During the upward and downward motion we expect a negative (downward as g) acceleration, constant and less than g.

The behavior of the position versus time is qualitatively the expected one: the plot seems to be made of parabolic branches (Fig. 9A). But on looking at the velocity, we see that it does not have the predicted constant slope during the upward and downward motion (Fig. 9B) This is apparent also in the acceleration-versus-

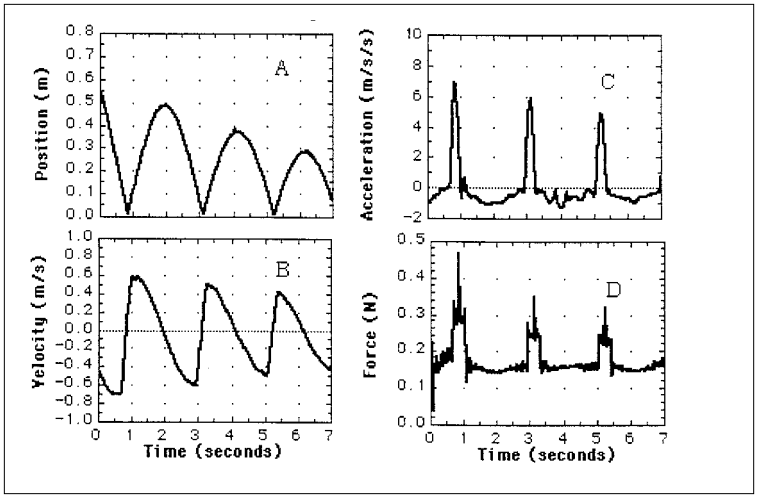

Fig. 9.

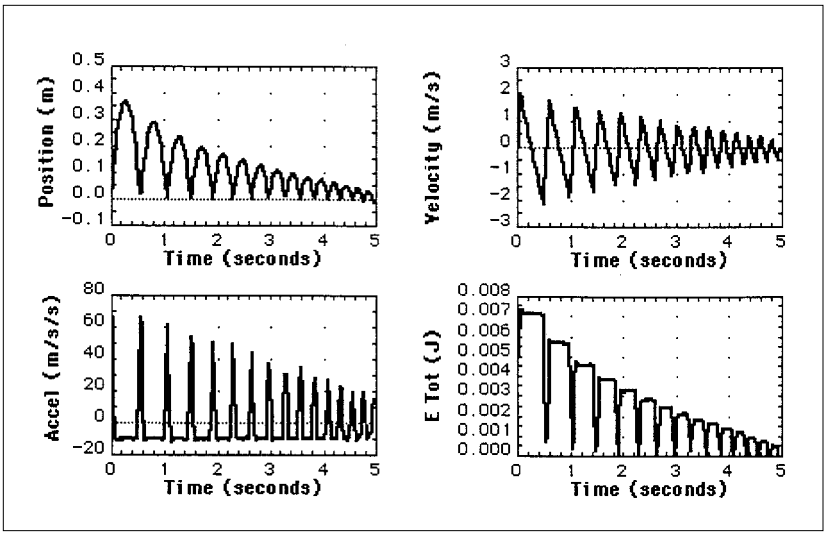

Fig. 10.

time plot that shows *modulations* even far from the instants when the yo-yo bounces back (Fig. 9C). We also notice that the absolute value of the acceleration *is minimum when the string is almost completely wound off*.

How do we explain this modulation? A possible explanation is that the effective radius of the axis changes because the string winds over itself and this acts like an axis with increasing diameter. In other words when the string is almost all wound up on the axis (velocity ≈ 0, and the yo-yo in the topmost position), the effective radius of the axis is larger than the r value that our model assumes. The Maxwell wheel can therefore be introduced as a refined version of the toy, intentionally designed in order to avoid the difficulties met in the yo-yo investigation. It may also be stimulating for the students to realize that, as hinted before, the graphs of the kinematic description of the motion of the wheel closely resemble those of the motion of a bouncing ball.

In Fig. 10 we report experimental data collected with a position sensor located above a Ping-Pong ball bouncing on the floor (the ball position is nevertheless recorded as distance from the floor, in order to allow easier comparison with the previous graphs).

The motion is weakly damped by viscous forces: the acceleration differs only by 1% from g ($a \approx 9.7$ m/s^2). We may also calculate here the total energy, (E_{tot}) as the sum of the potential energy ($U = mgx$) and the kinetic energy ($E_c = mv^2/2$) (the ball mass is $m = 2g$). We see that the energy is nearly constant during the upward-downward motion; the energy loss takes place essentially during the collision, where the kinetic energy is converted into elastic energy (peaks toward $E = 0$). This elastic energy is partially given back as kinetic energy after the collision, and partially dissipated as sound (mechanical energy leaving the ball) and heat (increasing the temperature of the ball and the ground).

Comments

We suggest that by interfacing the Maxwell wheel with a PC we can transform a lab experience into a fruitful opportunity not only to strengthen students' knowledge of mechanics but also to emphasize the role of the models in constructing physics knowledge. The data acquisition system can be a powerful cognitive tool. It allows a real-time visualization of the relevant variables selected by students according to any particular model they wish to test, and encourages them to play the game of gradually refining the apparatus in order to reach a satisfactory agreement with experimental data. Furthermore, the opportunity offered by the system to easily compare descriptions of different phenomena and to detect common and uncommon features may help students to better appreciate the potentialities of the kinematic description of motion.

References and Notes

1. With the two strings attached to a single point, they will spirally wind around the axis, thereby avoiding changes in the effective radius r.
2. Produced by Vernier Software, Portland OR, www.vernier.com.
3 Produced by PASCO scientific, Roseville, CA, www.pasco.com.
4. The noise on acceleration data is due to the effect of the double derivative of position data.
5. We may reach the same result by equating the torque T, applied by the external force, to the derivative of the angular momentum dL/dt. If we calculate the momenta with respect to the axis of symmetry of the wheel, the driving torque is $T = r\tau$, where τ is the sum of the vertical components of the string tensions (the gravitational force mg, applied to the center of mass, has zero momentum). The angular momentum is $L = I\omega$, and therefore $r\tau = I\mathrm{d}\omega/\mathrm{d}t = I(a/r)$, which gives the tension $\tau = aI/r^2$. Using Newton's second law for the net force $mg - \tau$ applied to the wheel, we get the equation $ma = mg - \tau = mg - aI/r^2$. Solving with respect to a we obtain: $a = g[m/(I/r^2 + m)] = g/k$.
6. The glitch in the plot $\tau(t)$ at the beginning of the fall is due to the scissors cutting the string.